

CRISPnet: Color Rendition ISP Net

Matheus Souza and Wolfgang Heidrich

King Abdullah University of Science and Technology (KAUST),
Thuwal, Saudi Arabia

`{matheus.medeirosdesouza,wolfgang.heidrich}@kaust.edu.sa`

Abstract. Image signal processors (ISPs) are historically grown legacy software systems for reconstructing color images from noisy raw sensor measurements. They are usually composed of many heuristic blocks for denoising, demosaicking, and color restoration. Color reproduction in this context is of particular importance, since the raw colors are often severely distorted, and each smart phone manufacturer has developed their own characteristic heuristics for improving the color rendition, for example of skin tones and other visually important colors.

In recent years there has been strong interest in replacing the historically grown ISP systems with deep learned pipelines. Much progress has been made in approximating legacy ISPs with such learned models. However, so far the focus of these efforts has been on reproducing the structural features of the images, with less attention paid to color rendition.

Here we present CRISPnet, the first learned ISP model to specifically target color rendition accuracy relative to a complex, legacy smart phone ISP. We achieve this by utilizing both image metadata (like a legacy ISP would), as well as by learning simple global semantics based on image classification – similar to what a legacy ISP does to determine the scene type. We also contribute a new ISP image dataset consisting of both high dynamic range monitor data, as well as real-world data, both captured with an actual cell phone ISP pipeline under a variety of lighting conditions, exposure times, and gain settings.

Keywords: image signal processor; image restoration; color rendition.

1 Introduction

The past decade has seen tremendous progress in miniaturizing camera modules to fit high quality imaging systems into flat mobile devices. As this miniaturization effort is approaching physical limits, such systems increasingly rely on computational methods to maintain high image quality. Image Signal Processors (ISPs) are responsible for tasks such as interpolation, demosaicking, denoising, enhancement on the edges, white balancing and color restoration, exposure correction, gamma encoding, compression, and so forth. The increasing miniaturization places a higher burden on these tasks, and in particular the reproduction of accurate colors. For example, the pixel pitch in modern smart phone cameras

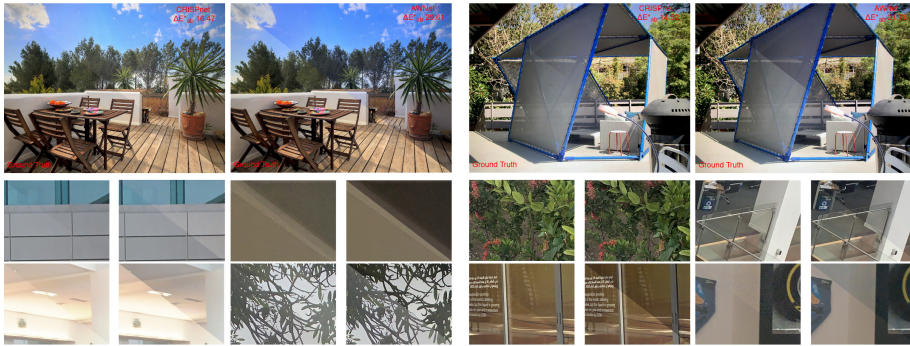


Fig. 1. Examples of faithful color rendition produced by CRISPnet compared to AWNet [6] for two full images and several image patches. The lower triangle in each image is the ground truth, the upper triangle is the respective learned model. Within each pair, the left result is CRISPnet, the right AWNet. Note also the quantitative improvement in ΔE_{ab}^*76 (lower is better).

is now as small as $0.7 \mu\text{m}$ – barely larger than one wavelength of red light¹, leading to significant crosstalk between the pixels in a Bayer pattern image [1]. This distortion is a spectral effect that can not be accurately modeled as a simple deconvolution or color matrix in RGB space.

Existing ISPs combat such image artifacts with complex, historically grown pipelines made up of heuristic blocks that are prone to error accumulation through the pipeline. At the same time, these systems are based on substantial expertise in color theory and human perception, and lead to a brand-specific “look” that accounts for a lot of the appeal of particular smart phone models.

In recent years there have been a number of proposals for replacing the historically grown and heuristic ISP pipelines with simpler, more principled approaches. Initially, these efforts relied on optimization-based approaches [13], but with increasingly more powerful compute resources [17] the attention has now shifted to deep learning and convolution neural networks (CNNs) [29,32]. More recent efforts include PyNET [16] and similar methods [14,20,6] that train ISP networks to match DSLR data.

We believe this approach is fundamentally limited in that **DSLRs can not be considered the gold standard in color processing**: while DSLRs have superior optics and noise characteristics, they have very minimalistic ISPs, and effectively offload the problem of color rendition to the end user – typically a professional photographer who will manually post-process the images in photoshop or similar tools.

In this work we therefore propose a learned ISP framework that leverages in particular the color science expertise that has gone into the development of legacy smart phone ISPs. Color Rendition ISP Net (CRISPnet) is trained on pairs of raw and ISP-processed smart phone images. In addition, it also learns

¹ e.g. Samsung ISOCELL sensors

to leverage the same white balance metadata that also informs the legacy ISP pipelines. Finally, like many legacy ISPs, CRISPnet performs a rough semantic image analysis, for example to distinguish between landscape and portrait shots. We show that each of these architectural improvements significantly increases reconstruction accuracy, especially with respect to color rendition. In summary, we make the following contributions:

- a novel deep architecture for ISP processing specifically tailored at matching the color processing of legacy ISPs.
- a way to inject white balance metadata into the network so that it can learn to be robust under different illuminations and scenes.
- an attention-based image semantics module that helps the ISP net to make different decisions for different scene types.
- an extensive new dataset for ISP networks consisting of pairs of raw and ISP processed smart phone camera images over a wide range of exposure and gain settings. The dataset consists of two parts – a large monitor dataset captured from a color calibrated HDR monitor (used for large scene diversity), and a smaller real-world dataset used for fine tuning.

Code and data will be made available.

2 Related Work

The idea of treating all stages involved in an ISP pipeline as a single integrated problem was proposed in [13]. Their framework takes the traditional modular structure applying different heuristics in each stage and substituted it with a single inverse problem. The proposed approach uses proximal operators and the primal-dual method for optimization, performing all of that together with various natural image priors (BM3D [5], TV, and cross-channel [12]). However, these natural image priors are relatively weak compared to modern deep learned models, leading to a degradation in image quality.

Later the optimization strategies were substitute by deep learning methods, building on excellent results reported for in image processing tasks like denoising [40,30,39,3], deblurring [37,25,4], super-resolution [35,26,7,21], etc. These systems focused on solving denoising and demosaicking jointly, learning mappings from raw to sRGB and from sRGB to raw [2,38]. Although these works can diminish noise, the color fidelity is sometimes left behind.

Other works on deep learned ISPs were focusing on image enhancements. Schwartz et al. [32] proposed a DeepISP mapping from a low-light mosaicked image to final sRGB, while Igantov et al. [16] proposed PyNET, targeting translation of mobile raw images to match the quality DSLR sRGB. After PyNET, more architecture ideas emerged [18,15], the most competitive ones relying on encoding-decoding structure with backbone resembling network like ResNET, UNet, Pix2Pix, etc. [11,31,19] often combined with attention mechanisms [14,20,6], these models further increase the accuracy, exploiting global and local features, applying spatial and channel attention similar to [36] proposed.

However, all these works have adopted the notion of training a mapping between mobile raw data and DSLR color images. While DSLRs have superior optics and sensors, they mostly rely on the user to post-process the image to improve the color rendition, while the ISPs of smart phones and point-and-shoot cameras are optimized to produce good looking final color images without manual post-processing. As a result many consumer camera tests now consider mobile camera images to have better color rendition than DSLRs without post-processing.²

In this work we therefore aim to leverage the substantial expertise in color theory and human perception that has flown into legacy ISP pipelines, and train a network to reproduce the color processing of a legacy smart phone ISP. Since such ISP pipelines make many non-linear and scene-dependent decisions, we show that this mapping can not be learned effectively with previous ISP network architectures. We therefore propose two architectural improvements: first, we utilize image meta data captured with the raw data. Image meta data was previously used in tone mapping applications [28], but it also is used extensively in traditional ISP pipelines. In this work, we specifically utilize white balance information to learn an ISP network with improved color rendition. We note that the use of white balance information differs from the previously proposed use of the color matrix metadata [22], since the color matrix is a scene-independent characteristic of the camera hardware, while the white balance data is scenes-specific. We also propose a global feature learning approach to feed scene composition and semantics information into the ISP process. For this purpose, we adopt the new XCiT transformer architecture [10], which we found to work better for this purpose than alternatives like Swin transformers [24].

As mentioned above, the most commonly used dataset for ISP networks uses pairings of mobile and DSLR images [16], and is therefore not of use for our system. Other existing datasets (e.g. [32]) are too small to really benefit our method. We therefore also propose a new dataset with a mix between HDR monitor captures and real world data. The HDR monitor data provides large scene diversity with excellent dynamic range and color calibration but is limited by the resolution of the monitor, which is lower than that of the camera. The real world data is used for fine tuning the recovery of pixel-level details, but cannot match the scene diversity of the monitor data.

3 Method

The ISP problem can be interpreted as an image translation task. Given a raw image, we want to learn a mapping to RGB that maintains the characteristics of the original device. Therefore, during this process, the method must learn low-level and high-level properties such as denoising, deblurring, sharpening, white balance, etc. The recent ideas provide end-to-end solutions mainly focusing on denoising and demosaicking [38,2,32]. However, in modern ISP pipelines, the

² e.g. <https://www.photographyacademy.com/why-phones-take-better-pictures-than-your-dslr>

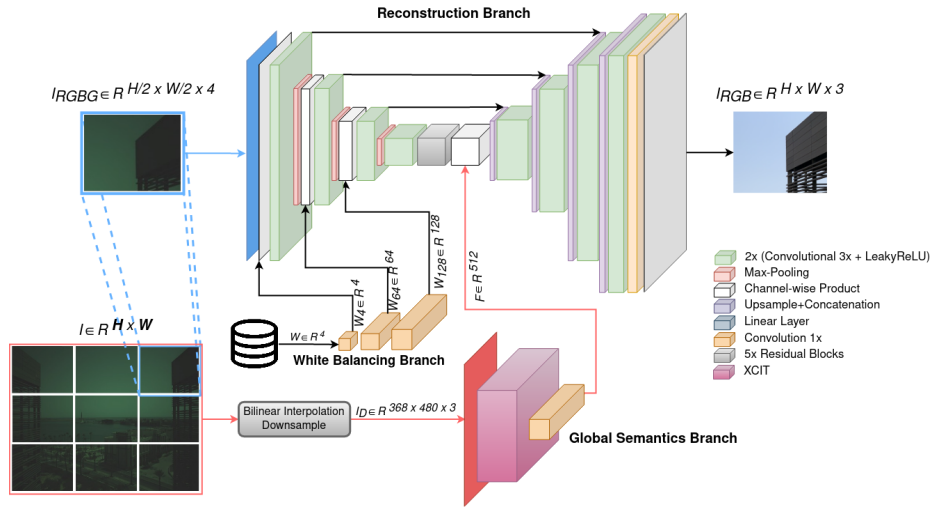


Fig. 2. An illustration of the CRISPnet. It receives as input the image divided into patches, the full image downsampled to 368×480 pixels, and the white balancing metadata. Here, \mathbf{H} and \mathbf{W} represent the full image dimension, while H and W is the dimension of the image patches. W represents the white balance value for each image channel. The network is divided into three branches. The reconstruction branch is responsible for overall image reconstruction while aggregating information from the other branches efficiently. The white balance branch projects the white balance information to match the layer dimension inside the reconstruction and the global semantics branch learns global scene semantics from a downsampled version of the full image. a) and b) correspond to two different strategies explored in this work.

white balance and the global scene classification heavily influence the final result and will be explored in the following.

CRISPnet follows the architecture shown in Fig.3. The Bayer raw image $I \in \mathbb{R}^{H \times W}$ goes through two branches. The reconstruction branch restructures the Bayer mosaic I into a 4 channel image $I_{RGBG} \in \mathbb{R}^{\frac{H}{2} \times \frac{W}{2} \times 4}$. Tiles of this image are processed with a modified UNet, which is also responsible for aggregating information from the other branches. The output of the reconstruction branch are ISP processed tiles that are reassembled into a translated RGB image $I_{RGB} \in \mathbb{R}^{H \times W \times 3}$.

The second branch operates on a downsampled version of the full image $I_D \in \mathbb{R}^{480 \times 368}$ with fixed resolution. This branch is responsible for learning global semantics when the training images are divided into patches. The output of this branch $F \in \mathbb{R}^{512}$ matches the dimensions of the bottleneck in the reconstruction branch and the two branches are combined with a channel-wise product.

Finally, we also inject image meta data into the reconstruction branch at three separate stages, again through a channel-wise product. The meta data consists of white balance information – three channel weights that are processed

through a third network branch. We also experimented with additional meta data such as exposure time and gain, but did not find them useful in improving the results. On the other hand, a learned injection of the white balance data does show significant improvements compared to both not using meta data at all and also compared to simple pre-multiplication of the white balance weights on the input data (see Section 5).

3.1 Reconstruction Branch

The backbone of CRISPnet has a UNet structure Fig.3, which has proved to be effective for this task by many of the works proposed in [18,15]. Its fully convolutional structure enables efficient inference for high resolution images. Like other learned ISPs, we perform patch-based image processing in order to control the computational expense for training the network. Our implementation has three main differences when compared with “vanilla” UNet proposed by [31]. Here we want to aggregate additional information in order to reconstruct faithful colors.

In legacy ISP pipelines white balance information is taken into account in several stages. To reproduce this behavior, we aggregate this information in the early layers using the white balance branch output as scales for the first three downsample levels in the network. Different ideas were proposed to better perform feature matching, including concatenation, dot-product, as well as more complex solutions like [27]. However, as detailed below, since the white balance branch is based on a small number of inputs, a simple projection works best for this purpose.

After aggregating the ambient light information exploiting white balance data, we add residual blocks in the bottleneck. Mixing ideas from ResNET and UNet is not new; [8,41] explored the power of both architecture together. In this work, we also exploit this, using the residual blocks only in the network bottleneck, as Fig.3 illustrates. For our application we observed that residual blocks in the encoder part lead to overfitting.

Finally we inject global features from the scene learned by the implicit global semantics branch. We take advantage of the compressed representation after the residual bottleneck to match the global features $F \in \mathbb{R}^{512}$. We experimented with a number of injection strategies, but finally adopted a channel-wise product, which scales the information inside the bottleneck channels, increasing or diminishing the impact of feature channels in the final reconstruction.

3.2 White Balance Awareness

The raw file contains unprocessed or minimally processed data as well as image metadata that describes image characteristics and parameters chosen by the device during the shot, based on light conditions or user preferences. Traditional raw to RGB solutions take advantage of this data but most current Deep Learning models ignore it.

The standardized metadata in a DNG file includes parameters such as a color matrix, white balance weights, as well as exposure and ISO settings. Of these, the color matrix describes the camera hardware but not the specific image; as such it is easy to implicitly pick up for a neural network just based on image pairs without explicitly using the metadata information. Similarly, we experimentally found that ISO and exposure settings do not improve the ISP reconstruction task. The situation however is very different for the white balance data – here we notice a substantive improvement by injecting this type of metadata into the learning process.

The white balance meta data comes in the form of one scalar multiplier per color channel, where the green channel is usually normalized to a value of 1. We expand this information to $W \in \mathbb{R}^4$ in RGBG format. Learned convolutional layers then upsample this information to the same size as the corresponding layers in the reconstruction branch so that the white balance information can be injected into the reconstruction branch at three distinct locations with a channel-wise dot product.

Note that the white balance branch does not contain any activation functions – since the input is only three scalars, and no scene information is available, we did not find it helpful to include non-linearities in this branch. Instead, the information is simply injected into the reconstruction branch, which can then learn how to best merge the information from the image and the meta data.

In Section 5 we show that this *learned* utilization of metadata is superior to the naive approach of just pre-multiplying the image with the three scalars. We also show in the ablation studies that three injection points are a sweet spot to balance image quality and network complexity.

3.3 Global Semantics Branch

Unlike the ISPs in DSLRs, the legacy ISPs in mobile phones and point-and-shoot cameras perform highly scene dependent image processing to produce good looking images without manual intervention. Different scenes (e.g. indoor vs. outdoor, portraits vs. landscapes) and conditions (e.g. sunny vs. overcast, snowy vs. green) may require different color adjustments to produce appealing final images. Reproducing this behavior is extremely hard because ISPs are closed software, and is not straightforward to infer how all the high level and low level image processing blocks work inside.

Deep learning models have the power to learn global semantics, and attention mechanisms have proven to work particularly well for this purpose. Previous works [6,14,20] apply attention mechanisms to capture the relation between objects, however since they work on patches, they have no access to the global scene semantics. To address this issue, CRISPnet has a specialized branch to deal with global semantics, exploiting the efficient transformer architecture XCiT [10] to extract and combine global features. We also discuss alternative ideas that we experimented with.

Different from the reconstruction branch, this branch takes as input the full raw image $I \in \mathbb{R}^{H \times W \times 4}$, downsampled to $I_D \in \mathbb{R}^{368 \times 480 \times 3}$. While the main

reconstruction branch is convolutional and can operate either on patches or full frame images, this branch therefore always operates on images of the same size, and has full access to the global semantics of the scene independent of patch cropping.

This empowers CRISPnet to exploit global scene semantics in the ISP reconstruction task. Specifically, we propose to exploit attention mechanisms in a different way from previous approaches with spatial and channel attention [14,20]. Here, we apply a transformer-based approach. Transformers are known for their large receptive field and hence the ability to learn global representations. The recent Cross-Covariance Image Transformers (XCiT) [10] has these benefits while remaining efficient; we therefore chose them as the core of our global feature branch.

The XCiT transformer, instead of having all tokens attending to all tokens, applies a “transposed” version of the ViT idea [9], where the features channels attend to other channels, making the complexity linear in the image resolution. In XCiT, the attention is computed using the cross-covariance between queries and key projections of tokens. This is motivated by the relationship between the Gram matrix and the covariance matrix, in which the eigenvalues of one can be obtained by decomposition of the other. This cross-covariance self-attention is followed by a local patch interaction and a feed-forward network. In CRISPnet, the “tiny” version of XCiT was simplified even more, reducing its depth to 4 – legacy ISP classification strategies are simple, and we did not want to overparameterize this branch.

The downsampled full image passes through these blocks, and the final representation is then aggregated using the final hidden state of the CLS token [34], which is commonly used for classification tasks. This sequence is projected using a 1x1 convolutional layer to match the bottleneck dimension of the reconstruction branch $F \in \mathbb{R}^{512}$. Finally, the features are combined using a channel-wise product.

This pipeline produces consistent results between patch-based and full-frame inference. As Section 5 shows empirically, learning full image global representations substantially improves the reconstruction accuracy.

In earlier versions of CRISPnet, we also experimented with alternative ways to extract global semantics. For example, we tried an architecture resembling a simple classification network, where the downsampled raw image passes through strided convolution followed by batch normalization and ReLU, and then a max pooling layer. This process was repeated twice and lastly, a fully connected layer was applied to encode the information to $F \in \mathbb{R}^{512}$. We matched this compressed representation with the reconstruction branch bottleneck using a channel-wise product. Notice that we did not downscale the feature to the dimension of the label because they are not known. Instead, we implicitly learned the global features for the current image through the same loss function as the reconstruction branch. While this approach worked well overall, we observed more issues with noisily low light images, and instead adopted the XCiT model described above.

4 Dataset and Training

4.1 Dataset

To train CRISPnet, we require a large dataset of pairs of raw and ISP-processed mobile phone data. Existing datasets are not suitable for this task since they are either too small for our purposes [32], or use a DSLR as a reference camera [16].

We therefore captured our own dataset. Since global semantic scene information is crucial to our approach, we require a large diversity of different scene types. We therefore resort to a two-part dataset: a large database of monitor-captured images that cover a wide range of different environments, including indoor and outdoor, and different types of landscapes. In addition, we also capture a smaller real-world dataset that is used for fine-tuning to overcome any pixel artifacts that may occur due to the monitor data.

All data was captured using an iPhone XR and the ProCam software for IOS. Every shot using this app generates two images of size 4032×3024 : raw (DNG format) and RGB. The raw is a single channel grid (Bayer Pattern) with 16 bit values, which represents the measured light intensity. The RGB images are generated by passing the same raw images through the iPhone XR pipeline.

Monitor data. The monitor captures were performed in a dark room using the CG3145 4K HDR monitor. This monitor has a typical contrast ratio of 1,000,000:1, which it achieves with a dual modulation principle [33]. However, unlike most dual modulation HDR monitors that use an LCD illuminated by a low-frequency LED backlight [33], the Eizo CG3145 actually uses two LCD layers stacked on top of each other on the same glass substrate. This allows the monitor to achieve not only high global contrast, but also excellent local contrast of high frequency features. As such, it is capable of producing high quality images over a large range of intensities, as well as individual images that exceed the dynamic range of the mobile phone camera to simulate challenging illumination conditions. The monitor was color calibrated using off the shelf software for accurate representation of the source material.

Using a tripod-mounted phone setup and a capture script, we acquired a total of 2000 raw/ISP image pairs. The source material was taken from [23] as well as from a new HDR portrait dataset.³

Real world data. One downside of the monitor setup is that the screen resolution of $4,096 \times 2,160$ is lower than the resolution of the mobile phone camera, which introduces pixel level artifacts. To combat these, we also capture a real world dataset for fine-tuning the training. This dataset has accurate pixel-level details, but much lower scene diversity than the monitor data, since it is not feasible to travel to remote places to capture images in different sites. All in all, we captured 200 real world image pairs.

³ Details will be provided in the final version to preserve double blindness.

4.2 Training

From the monitor dataset we select 750 images (600 for training, 75 for testing, and 75 for validation) and from the real-world dataset 198 images (160 for training, 19 for testing, and 19 for validation). The idea here is to first train using only monitor data and then fine-tune with the real-world. A small crop was performed on the monitor data to avoid capturing the bezel of the monitor itself, reducing the resolution from 4032×3024 to 3840×2944 . Next, each picture was divided into 64 patches of 368×480 to train the reconstruction part. While the reconstruction receives a patch, the global feature acquisition branch is fed with the downsampled as discussed above.

4.3 Loss Function

In our experiments we adopted the MSE loss function. Usually in this field, “perceptual” and SSIM losses are used together with MSE or MAE. However, we did not observe sufficient improvements from these losses to justify the increased training overhead. We also note that these alternative losses focus on structural image features and tend to neglect color reproduction. In the supplementary material we provide a more detailed analysis.

5 Experiments



Fig. 3. Full frame image reconstruction after fine-tuning CRISPnet to deal with real-world data, compared against AWNet [6]. CRISPnet is able to reproduce the light condition in the scene and therefore producing accurate colors.

For comparison with the state-of-the-art, we re-train several SOTA methods on the same dataset described above. The chosen methods we compare with are AWNet [6], PyNET CA [20] and CSANet [14]. All these strategies are improvements over PyNET [16] and the best reported results in Mobile ISP contests [18,15]. All three methods were trained using our dataset following the technical recommendations, parameters, and loss functions described by them. AWNet and PyNET CA provided code and CSANet was implemented by ourselves. The strategy of training with monitor data and then using the real-world to fine-tune was performed for them as well. CRISPnet is also compared against the UNet with residual bottleneck, which is our network backbone without the global feature acquisition and white balance branches.

To assess the color rendition accuracy we use the ΔE_{ab}^*76 metric, which is the RMS error in the non-linear, *perceptually uniform* CIELAB space. Perceptual uniformity means that the distance in the CIELAB space can be directly mapped to *just noticeable differences* (JND) between two similar colors. Specifically, one JND corresponds to $\Delta E_{ab}^*76 \approx 2.3$, so that two colors that differ by this value can just barely be distinguished by a standard human observer. We also adopted the standard PSNR and SSIM metrics.

Method	PSNR \uparrow	ΔE_{ab}^*76 \downarrow	SSIM \uparrow
CSANET [14]	24.51	16.07	0.8631
PYNET CA [20]	25.00	15.50	0.8561
AWNET [6]	25.70	14.41	0.8947
UNet + Residual Bottleneck	26.33	13.76	0.9130
CRISPnet	27.54	11.75	0.8911

Table 1. Reconstruction results on Real-World dataset first fine-tuning using Monitor data.

Table 1 shows quantitatively our final result evaluated with real-world data after fine-tuning. CRISPnet provides a substantial increase in terms of PSNR and ΔE_{ab}^*76 over our comparisons. We can observe how the other methods suffer to translate faithful colors and how relying only on PSNR and SSIM does not reflect the color rendition. In particular the SSIM is too focused on structural similarity and overlooks color discrepancies that are very noticeable in Fig.3. When only monitor data training is taken into account the metrics are higher overall (Table 2). For this case, we have a larger dataset, with captures done always in the same camera positioning settings, and the monitor resolution is lower than the camera, these facts make the reconstruction task easier. CRISPnet proves to better exploit these characteristics and outputs better results in all evaluated metrics. Fig.1 shows qualitatively that our model is almost indistinguishable from the Ground Truth, while AWNet cannot translate colors precisely.

5.1 Ablation Studies

Tables 1 and 2 show how each proposed improvement enhances the reconstruction process. Initially, we have a well-known UNet [31] with residual connection

Method	PSNR \uparrow	ΔE_{ab}^*76 \downarrow	SSIM \uparrow
CSANET [14]	27.05	11.43	0.8986
PYNET CA [20]	27.41	11.06	0.8796
AWNET [6]	27.66	10.84	0.9093
UNet + Residual Bottleneck	28.34	10.25	0.9243
CRISPnet	32.04	6.36	0.9344

Table 2. Reconstruction results on Monitor dataset. This is considerer in our pipeline a pre-training step to finally fine-tune for Real-World data.

in the bottleneck. Next, we introduce the white balance (WB) information, Table 3 ablates over not using metadata at all, naively using white balance information as preprocessing step, and finally using the proposed branch with the UNet with residual bottleneck. We can observe quantitatively its importance and Fig.4 clarify this even more. Through Table 3 we empirically justify our design choice of injecting white balancing information at three points. We also show that preprocessing the images with metadata for AWWNet [6] is not effective as our proposed branch – Table 3 makes this clear.

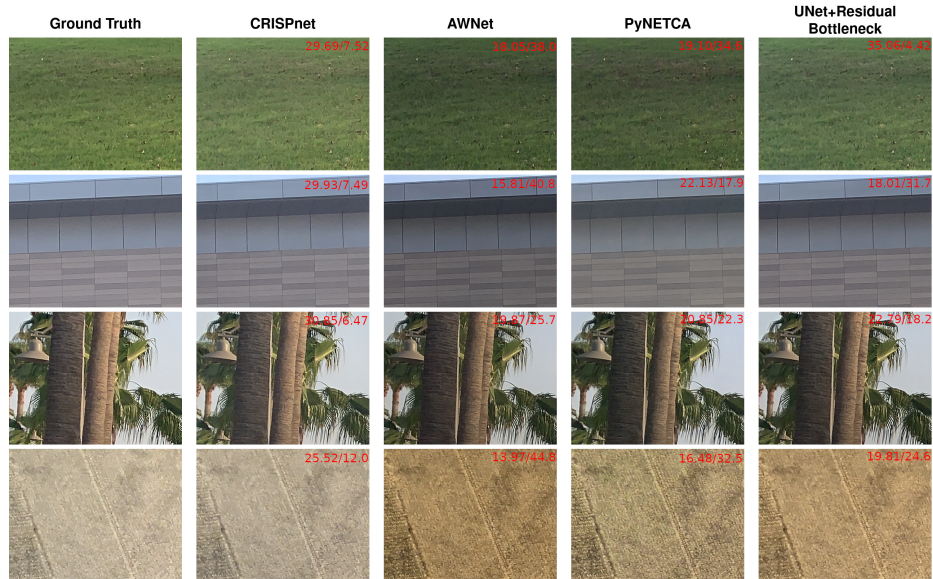


Fig. 4. CRISPnet compared against AWWNet, PyNET CA and our backbone (UNet+Residual Bottleneck). PSNR/ ΔE_{ab}^*76 .

We also ablate about the importance of training first with monitor data and then fine-tune with real-world. The additional branches of CRISPnet make it powerful enough to learn color conditions that can be heavily refined during

Method	PSNR \uparrow	ΔE_{ab}^*76 \downarrow	SSIM \uparrow
AWNet [6]	27.66	10.84	0.9093
AWNet [6] Preprocess WB	28.51	9.88	0.9113
No WB	28.34	10.25	0.9243
Preprocess WB	28.98	9.57	0.9236
Branch level 1	29.84	8.42	0.9261
Branch level 1, 2 and 3	29.86	8.40	0.9281
Branch level 1, 2, 3 and 4	29.75	8.48	0.9264
Branch level 1, 2, 3, 4 and 5	29.69	8.56	0.9256

Table 3. Comparison of different ways to explore the White Balance (WB) information. AWNet is slightly improved by preprocessing the input with white balance metadata. However, it still behind our results even before the global semantics branch been added.

fine-tuning. If we train CRISPnet only with monitor data and reconstruct real-world scene our PSNR, for instance, stays around 23.9 dB, after fine-tuning it increases beyond 27.5 dB. Table 4 shows what happens when we train straight using real-world data for both CRISPnet and the UNet with residual bottleneck. Comparing against Table 1 we can notice that for all metrics the results are degraded. Therefore, our proposed dataset attached with the fine-tune strategy enables better output without the requirement of taking thousands of real-world image pairs.

Method	PSNR \uparrow	ΔE_{ab}^*76 \downarrow	SSIM \uparrow
UNet + Residual	26.03	14.14	0.9038
CRISPnet	26.73	12.51	0.8746
CRISPnet Fine-tuned	27.54	11.75	0.8911

Table 4. Result on the Real-World data without and with fine-tuning process.

Finally, we observe the impact of global semantics branch and the different ways to do it. CRISPnet extracts the global semantics information through an XCiT transformer model [10], which is a more powerful attention mechanism than traditional spatial or channel attention. Table 5 shows quantitatively that exploiting global semantics indeed improves the reconstruction quality and a light transformer-based attention mechanism beats a simple CNN approach for this purpose. More ablations about different attention mechanisms and how CRISPnet performs with deeper XCiT models are available in the supplementary material.

6 Discussion, Limitations, and Future Work

In this work we introduced CRISPnet, the first ISP network designed to improve color rendition by learning from the expertise encoded in legacy ISP

Global Semantics	Monitor			Real-World		
	PSNR \uparrow	$\Delta E_{ab}^*76\downarrow$	SSIM \uparrow	PSNR \uparrow	$\Delta E_{ab}^*76\downarrow$	SSIM \uparrow
Without	29.86	8.40	0.9281	26.80	13.01	0.9133
Classification CNN	31.89	6.55	0.9311	26.90	12.62	0.8874
XCiT	32.04	6.36	0.9344	27.53	11.75	0.8911

Table 5. Comparison between different global semantics strategies and its contribution.

pipelines. We achieve this by combining a convolutional encoder/decoder architecture for the main reconstruction task with both white balancing metadata and a transformer-based global feature branch. We demonstrate substantial improvements in both traditional image metrics (PSNR, SSIM), as well as color accuracy (ΔE_{ab}^*76).

However, the proposed approach is not without shortcomings. As can be seen from both the quantitative and the qualitative results, the color rendition is much improved, but often still not below the noticeable threshold. This indicates that legacy ISPs are still more complex than the existing network architectures are capable of reproducing. Furthermore, while our architecture improves color rendition, it can have sometimes have issues with noise especially in very low light. As shown in Figure 5, the color improvements usually still outweigh the poorer noise performance for an overall increased PSNR.



Fig. 5. For very low light images, our method can have more issues with noise than AWNet. However, the significant improvement in color rendition still results in an overall increased PSNR for CRISPnet. PSNR/ ΔE_{ab}^*76 .

Despite the low-light issue we believe that our approach is preferable in many situations – global color distortions are often significantly more noticeable than fine scale noise in typical use cases for the images (e.g. when the images are posted on social media in lower resolution anyways).

In the future it would be interesting to explore how to improve the noise performance, for example by having both a DSLR reference image to improve the structural details of the image and a mobile phone ISP image for the color rendition. Ultimately it would be best if we did not require a reference ISP algorithm at all and could instead learn to reproduce the manual color adjustments made by skilled professional photographers. We believe the architectural changes we propose in this paper can also be useful for these types of systems.

References

1. Anzagira, L., Fossum, E.R.: Color filter array patterns for small-pixel image sensors with substantial cross talk. *JOSA A* **32**(1), 28–34 (2015)
2. Cao, Y., Wu, X., Qi, S., Liu, X., Wu, Z., Zuo, W.: Pseudo-isp: Learning pseudo in-camera signal processing pipeline from a color image denoiser (2021)
3. Chang, M., Li, Q., Feng, H., Xu, Z.: Spatial-adaptive network for single image denoising (2020)
4. Cho, S.J., Ji, S.W., Hong, J.P., Jung, S.W., Ko, S.J.: Rethinking coarse-to-fine approach in single image deblurring (2021)
5. Dabov, K., Foi, A., Katkovnik, V., Egiazarian, K.: Image denoising by sparse 3-d transform-domain collaborative filtering. *IEEE Transactions on Image Processing* **16**(8), 2080–2095 (2007). <https://doi.org/10.1109/TIP.2007.901238>
6. Dai, L., Liu, X., Li, C., Chen, J.: Awnet: Attentive wavelet network for image isp (2020)
7. Dai, T., Cai, J., Zhang, Y., Xia, S.T., Zhang, L.: Second-order attention network for single image super-resolution. In: *Proceedings of the IEEE/CVF Conference on Computer Vision and Pattern Recognition (CVPR)* (June 2019)
8. Diakogiannis, F.I., Waldner, F., Caccetta, P., Wu, C.: Resunet-a: A deep learning framework for semantic segmentation of remotely sensed data. *ISPRS Journal of Photogrammetry and Remote Sensing* **162**, 94–114 (Apr 2020). <https://doi.org/10.1016/j.isprsjprs.2020.01.013>, <http://dx.doi.org/10.1016/j.isprsjprs.2020.01.013>
9. Dosovitskiy, A., Beyer, L., Kolesnikov, A., Weissenborn, D., Zhai, X., Unterthiner, T., Dehghani, M., Minderer, M., Heigold, G., Gelly, S., Uszkoreit, J., Houlsby, N.: An image is worth 16x16 words: Transformers for image recognition at scale (2021)
10. El-Nouby, A., Touvron, H., Caron, M., Bojanowski, P., Douze, M., Joulin, A., Laptev, I., Neverova, N., Synnaeve, G., Verbeek, J., Jegou, H.: Xcit: Cross-covariance image transformers (2021)
11. He, K., Zhang, X., Ren, S., Sun, J.: Deep residual learning for image recognition (2015)
12. Heide, F., Rouf, M., Hullin, M.B., Labitzke, B., Heidrich, W., Kolb, A.: High-quality computational imaging through simple lenses. *ACM Trans. Graph.* **32**(5) (oct 2013). <https://doi.org/10.1145/2516971.2516974>, <https://doi.org/10.1145/2516971.2516974>
13. Heide, F., Steinberger, M., Tsai, Y.T., Rouf, M., Pająk, D., Reddy, D., Gallo, O., Liu, J., Heidrich, W., Egiazarian, K., Kautz, J., Pulli, K.: Flex-isp: A flexible camera image processing framework. *ACM Trans. Graph.* **33**(6) (Nov 2014). <https://doi.org/10.1145/2661229.2661260>, <https://doi.org/10.1145/2661229.2661260>
14. Hsyu, M.C., Liu, C.W., Chen, C.H., Chen, C.W., Tsai, W.C.: Csanet: High speed channel spatial attention network for mobile isp. In: *Proceedings of the IEEE/CVF Conference on Computer Vision and Pattern Recognition (CVPR) Workshops*. pp. 2486–2493 (June 2021)
15. Ignatov, A., Chiang, C.M., Kuo, H.K., Sycheva, A., Timofte, R., Chen, M.H., Lee, M.Y., Xu, Y.S., Tseng, Y., Xu, S., Guo, J., Chen, C.H., Hsyu, M.C., Tsai, W.C., Chen, C.W., Malivenko, G., Kwon, M., Lee, M., Yoo, J., Kang, C., Wang, S., Shaolong, Z., Dejun, H., Fen, X., Zhuang, F., Ma, Y., Peng, J., Wang, T., Song, F., Hsu, C.C., Chen, K.L., Wu, M.H., Chudasama, V., Prajapati, K., Patel, H., Sarvaiya, A., Upla, K., Raja, K., Ramachandra, R., Busch, C., de Stoutz,

- E.: Learned smartphone isp on mobile npus with deep learning, mobile ai 2021 challenge: Report (2021)
16. Ignatov, A., Gool, L.V., Timofte, R.: Replacing mobile camera isp with a single deep learning model (2020)
 17. Ignatov, A., Timofte, R., Chou, W., Wang, K., Wu, M., Hartley, T., Gool, L.V.: Ai benchmark: Running deep neural networks on android smartphones (2018)
 18. Ignatov, A., Timofte, R., Zhang, Z., Liu, M., Wang, H., Zuo, W., Zhang, J., Zhang, R., Peng, Z., Ren, S., Dai, L., Liu, X., Li, C., Chen, J., Ito, Y., Vasudeva, B., Deora, P., Pal, U., Guo, Z., Zhu, Y., Liang, T., Li, C., Leng, C., Pan, Z., Li, B., Kim, B.H., Song, J., Ye, J.C., Baek, J., Zhussip, M., Koishekenov, Y., Ye, H.C., Liu, X., Hu, X., Jiang, J., Gu, J., Li, K., Tan, P., Hou, B.: Aim 2020 challenge on learned image signal processing pipeline (2020)
 19. Isola, P., Zhu, J.Y., Zhou, T., Efros, A.A.: Image-to-image translation with conditional adversarial networks (2018)
 20. Kim, B.H., Song, J., Ye, J.C., Baek, J.: Pynet-ca: Enhanced pynet with channel attention for end-to-end mobile image signal processing. *Lecture Notes in Computer Science* p. 202–212 (2020). https://doi.org/10.1007/978-3-030-67070-2_12, http://dx.doi.org/10.1007/978-3-030-67070-2_12
 21. Liang, J., Cao, J., Sun, G., Zhang, K., Gool, L.V., Timofte, R.: Swinir: Image restoration using swin transformer (2021)
 22. Liang, Z., Cai, J., Cao, Z., Zhang, L.: Cameranet: A two-stage framework for effective camera isp learning (2019)
 23. Lim, B., Son, S., Kim, H., Nah, S., Lee, K.M.: Enhanced deep residual networks for single image super-resolution. In: *The IEEE Conference on Computer Vision and Pattern Recognition (CVPR) Workshops* (July 2017)
 24. Liu, Z., Lin, Y., Cao, Y., Hu, H., Wei, Y., Zhang, Z., Lin, S., Guo, B.: Swin transformer: Hierarchical vision transformer using shifted windows (2021)
 25. Mao, X., Liu, Y., Shen, W., Li, Q., Wang, Y.: Deep residual fourier transformation for single image deblurring (2021)
 26. Niu, B., Wen, W., Ren, W., Zhang, X., Yang, L., Wang, S., Zhang, K., Cao, X., Shen, H.: Single image super-resolution via a holistic attention network (2020)
 27. Perez, E., Strub, F., de Vries, H., Dumoulin, V., Courville, A.: Film: Visual reasoning with a general conditioning layer (2017)
 28. Punnappurath, A., Brown, M.S.: Spatially aware metadata for raw reconstruction. In: *Proceedings of the IEEE/CVF Winter Conference on Applications of Computer Vision (WACV)*. pp. 218–226 (January 2021)
 29. Ratnasingam, S.: Deep camera: A fully convolutional neural network for image signal processing (2019)
 30. Remez, T., Litany, O., Giryes, R., Bronstein, A.M.: Deep class aware denoising (2017)
 31. Ronneberger, O., Fischer, P., Brox, T.: U-net: Convolutional networks for biomedical image segmentation (2015)
 32. Schwartz, E., Giryes, R., Bronstein, A.M.: Deepisp: Toward learning an end-to-end image processing pipeline. *IEEE Transactions on Image Processing* **28**(2), 912–923 (Feb 2019). <https://doi.org/10.1109/tip.2018.2872858>, <http://dx.doi.org/10.1109/TIP.2018.2872858>
 33. Seetzen, H., Heidrich, W., Stuerzlinger, W., Ward, G., Whitehead, L., Trentacoste, M., Ghosh, A., Vorozcovs, A.: High dynamic range display systems. *ACM Trans. Graphics* pp. 760–768 (2004)
 34. Touvron, H., Cord, M., Sablayrolles, A., Synnaeve, G., Jégou, H.: Going deeper with image transformers (2021)

35. Wang, X., Yu, K., Wu, S., Gu, J., Liu, Y., Dong, C., Loy, C.C., Qiao, Y., Tang, X.: Esrgan: Enhanced super-resolution generative adversarial networks (2018)
36. Woo, S., Park, J., Lee, J.Y., Kweon, I.S.: Cbam: Convolutional block attention module (2018)
37. Zamir, S.W., Arora, A., Khan, S., Hayat, M., Khan, F.S., Yang, M.H.: Restormer: Efficient transformer for high-resolution image restoration (2021)
38. Zamir, S.W., Arora, A., Khan, S., Hayat, M., Khan, F.S., Yang, M.H., Shao, L.: Cycleisp: Real image restoration via improved data synthesis (2020)
39. Zamir, S.W., Arora, A., Khan, S., Hayat, M., Khan, F.S., Yang, M.H., Shao, L.: Multi-stage progressive image restoration. In: Proceedings of the IEEE/CVF Conference on Computer Vision and Pattern Recognition (CVPR). pp. 14821–14831 (June 2021)
40. Zhang, K., Zuo, W., Gu, S., Zhang, L.: Learning deep cnn denoiser prior for image restoration (2017)
41. Zhang, Z., Liu, Q., Wang, Y.: Road extraction by deep residual u-net. *IEEE Geoscience and Remote Sensing Letters* **15**(5), 749–753 (May 2018). <https://doi.org/10.1109/lgrs.2018.2802944>, <http://dx.doi.org/10.1109/LGRS.2018.2802944>